npg

Autophagy within the antigen donor cell facilitates efficient antigen cross-priming of virus-specific CD8+ T cells

M Uhl[1,2,7], O Kepp[3,4,5,7], H Jusforgues-Saklani[1,2], J-M Vicencio[3,4,5], G Kroemer[3,4,5] and ML Albert*[,1,2,6]

Cross-presentation of cell-associated antigen is important in the priming of CD8+ T-cell responses to proteins that are not expressed by antigen-presenting cells (APCs). *In vivo*, dendritic cells are the main cross-presenting APC, and much is known regarding their ability to capture and process cell-associated antigen. In contrast, little is known about the way death effector pathways influence the efficiency of cross-priming. Here, we compared two important mechanisms of programmed cell death: classical apoptosis, as it occurs in wild-type (WT) fibroblasts, and caspase-independent cell death, which occurs with increased features of autophagy in *Bax/Bak$^{-/-}$* fibroblasts. We assessed virally infected WT and *Bax/Bak$^{-/-}$* fibroblasts as a source of cell-associated antigen. We found that immunization with cells undergoing autophagy before cell death was superior in facilitating the cross-priming of antigen-specific CD8+ T cells. Strikingly, silencing of *Atg5* expression inhibited priming. We interpret this to be a novel form of 'immunogenic death' with the enhanced priming efficiency being a result of persistent MHC I cross-presentation and the induction of type I interferons. These results offer the first molecular evidence that catabolic pathways, including autophagy, influence the efficiency of cross-priming. We predict that targeting the autophagy cascade may provide a therapeutic strategy for achieving robust cross-priming of viral and tumor-specific CD8+ T cells.
Cell Death and Differentiation (2009) **16,** 991–1005; doi:10.1038/cdd.2009.8; published online 20 February 2009

Multicellular organisms possess genetic and epigenetic mechanisms of programmed cell death (PCD) for the elimination of cells that are no longer needed or that have become damaged. Phagocytes engulf the dying cells, in turn maintaining tissue homeostasis. There is now evidence to suggest that antigen-presenting cells (APCs) have evolved mechanisms to capture immunologically relevant information from internalized apoptotic cells, thus offering a mechanism whereby cell death may influence subsequent immune response(s).[1–3] Specifically, it has been shown that antigen derived from phagocytosed dying cells may be processed by dendritic cells (DCs) to generate MHC I/peptide, resulting in the activation of CD8+ T cells. This pathway is called cross-priming due to the 'crossing' of the classically defined restriction of MHC I for presentation of endogenously synthesized protein.[4] In addition, dying cells are also capable of skewing cytokine production in phagocytes.[5] For example, macrophages and DCs engulf dying cells through specific phagocytic receptors (e.g., CD36, $\alpha_v\beta_5$, CR3 and others), which may result in the inhibition of proinflammatory cytokine secretion (e.g., IL-1β, IL-12 and TNF-α).[6–9] These studies have all addressed the downstream effects of dying cells on the immune system with little attention to the complexity of cell death pathways. We hypothesized that the molecular

mechanism of cell death influences the immunologic instruction given to the phagocyte and we focused our attention on two of the major classes of PCD that have been described: type I PCD (or classical apoptosis) and type II PCD (referred to as autophagic cell death or caspase-independent cell death).[10]

Distinct, yet intertwined pathways are involved in executing cell death programs. Briefly, apoptosis is mediated by caspases, a family of aspartic acid-specific proteases that initiate as well as execute the apoptotic process.[11] Caspases are synthesized as inactive precursors (zymogens) and are typically activated through proteolysis and oligomerization to become fully active. Activation of this pathway may come from extrinsic signals acting through surface receptors (e.g., FAS) or intrinsic signals that result in mitochondrial outer membrane permeabilization (MOMP) and release of cytochrome *c*. In many cell types, the extrinsic and intrinsic pathways converge on the family of BH3-only proteins, which are the candidate molecules responsible for Bax/Bak oligomerization in the mitochondrial outer membrane.[12] These pathways also intersect at caspase-3, which is directly cleaved by caspase-8 (the extrinsic pathway) and by caspase-9 following assembly of the apoptosome (the intrinsic pathway). Over the past 10 years, a caspase-centric view of PCD has emerged, in part due to the essential role for CED-3 in

C. elegans. Recent studies using caspase knockout mice or pan-caspase inhibitors offer a strikingly different perspective – evidence suggests that caspases are not necessarily required for achieving cell death in mammalian cells.[13,14]

Similar to apoptosis, caspase-independent cell death may be initiated by cell-surface death receptors or by DNA damage. One of the important forms of caspase-independent PCD has been referred to as autophagic cell death.[15] During normal cell aging and exposure to environmental stressors, autophagy does not lead to cell death; instead, it has a key function in cellular repair through the removal of damaged organelles. But when run in excess, due to protracted nutrient deprivation, hypoxia or infection, type II PCD may occur.[10] Specifically, the absence of signals from growth factors that signal through class I PI3K results in the inactivation of Akt/PKB and mTOR and may initiate autophagic death.[16] Alternatively, signaling through the class III PI3K/Vps34 complex, which contains beclin-1 (or Atg6), can initiate autophagy and subsequently cell death.[17] In both instances, the induction of autophagosomes occurs through the actions of two ubiquitin-like conjugation systems: LC3–phosphatidylethanolamine (LC3-PE) and Atg12–Atg5.[10] Following formation of the autophagosome, in part mediated by Rab7,[18] it fuses with the lysosome. Similar to apoptotic cells, phagocytes are responsible for the clearance of cells that die by autophagy, however the mechanisms of uptake are likely distinct.[19] As there exists some controversy as to whether cells are dying an autophagic cell death *per se*, or dying with features of autophagy, we will simply refer to this pathway as type II PCD or caspase-independent cell death with enhanced autophagy.

Our prior work revealed a central role for apoptotic cells in the delivery of antigen to DCs for cross-presentation and activation of CD8^{+} T cells.[2,6] This observation has been verified in multiple *ex vivo* and *in vivo* model systems; and it is the basis for ongoing immunotherapy trials in humans in which syngeneic DCs are pulsed with antigen-loaded apoptotic cells and re-infused into patients for the treatment of solid tumors (e.g., prostate cancer, melanoma). Herein, we examine how death effector pathways, as an upstream event, influence the efficiency of cross-priming. We show that *in vivo* immunization with cells undergoing autophagy is superior to apoptotic cells in facilitating the cross-priming of antigen-specific CD8^{+} T cells. Enhanced priming could be explained by two independent mechanisms: persistent TCR engagement due to a longer half-life for the MHC I/peptide complexes generated from the captured antigen; and the induction of type I interferons (IFNs) by cross-presenting DCs. Our findings may result in the identification of improved methods for therapeutically achieving cross-priming of viral and tumor-specific CD8^{+} T cells.

Results

Dendritic cells acquire antigen from dying cells and activate CD8^{+} T cells.

To compare type I and type II PCD, it was important to generate antigen-expressing cells that when induced to die use distinct death effector pathways. To restrict the numerous variables that might influence a DCs' ability to cross-present antigen, we chose to focus on genotoxic stress induced by UV-B irradiation, and employed genetically modified mouse embryonic fibroblasts (MEFs) as a strategy for controlling the mechanism of cell death. On the basis of prior studies, we chose to compare *Bax/Bak*^{−/−} and wild-type (WT) MEFs, with the former undergoing autophagy and dying a caspase-independent cell death as a result of being unable to initiate MOMP,[20,21] and the latter dying with features of classical caspase-mediated apoptosis. To load the respective cells with antigen, we chose to use influenza A infection as it is a robust system for monitoring both human and mouse CD8^{+} T-cell responses. As previously shown, influenza-infected cells are efficiently cross-presented for the activation of memory CD8^{+} T cells in humans, and can be used *in vivo* for the priming of naive CD8^{+} T cells in mice.[2,22]

To characterize our experimental system, we first confirmed that influenza-infected WT and *Bax/Bak*^{−/−} MEFs expressed similar amounts of viral antigen. Cells were washed out of serum-containing media and infected with 250 HAU per ml (MOI of 0.5) influenza A/PR/8 for 1 h at 37°C. Cells were washed with serum-containing media and incubated for an additional 4 h to allow for viral antigen expression. To monitor influenza nucleoprotein (NP) expression, cells were fixed, permeabilized, stained with anti-NP antibodies (Abs) and analyzed by FACS. As shown, there was comparable expression of NP in both the WT and *Bax/Bak*^{−/−} MEFs (Figure 1a). Evaluation of the expression of influenza matrix protein (M1) and hemagglutinin (HA) showed similar results (data not depicted). Further, we confirmed that during the first 6 h of caspase-mediated death, there is not selective destruction of NP (data not depicted). Next, we exposed cells to 120 mJ/cm^{2} of UV-B and monitored caspase-3 activation after 0, 8 and 24 h. This method of inducing death also served to inactivate the virus and prevent direct transfer of live influenza from the dying cells to the DC (data not depicted).

As expected, UV-B activated the apoptosome and triggered caspase-3 cleavage in the WT but not the *Bax/Bak*^{−/−} MEFs (Figure 1b). To confirm that the *Bax/Bak*^{−/−} MEFs were dying with biochemical features of autophagy, we screened cells for LC3 cleavage and p62 degradation.[23] In addition, we transfected the cells with a plasmid encoding an LC3-GFP fusion protein and monitored the presence of punctate LC3 staining on autophagosomes.[24] It was indeed possible to demonstrate biochemical and cellular evidence for autophagy in the *Bax/Bak*^{−/−} MEFs (Figure 1b and c). Interestingly, the WT MEFs manifested a mixture of autophagy and apoptotic cell death, however, there were significantly fewer LC3-GFP autophagosomes as compared to the *Bax/Bak*^{−/−} MEFs (see below and Supplementary Figure S2a). On the basis of these results, we determined that these matched cell lines (WT *versus Bax/Bak*^{−/−} MEFs) would permit us to compare the function of type I and type II PCD in facilitating the cross-presentation of antigen.

To investigate engulfment and cross-presentation by DCs, we used previously characterized assays for phagocytosis and T-cell activation.[6] PKH26 (red dye)-labeled MEFs were co-cultured with PKH67 (green dye)-labeled human monocyte-derived DCs and uptake was monitored by FACS analysis. As shown, the presence of double-positive cells indicated uptake by the DCs (Figure 2a). Addition of EDTA to
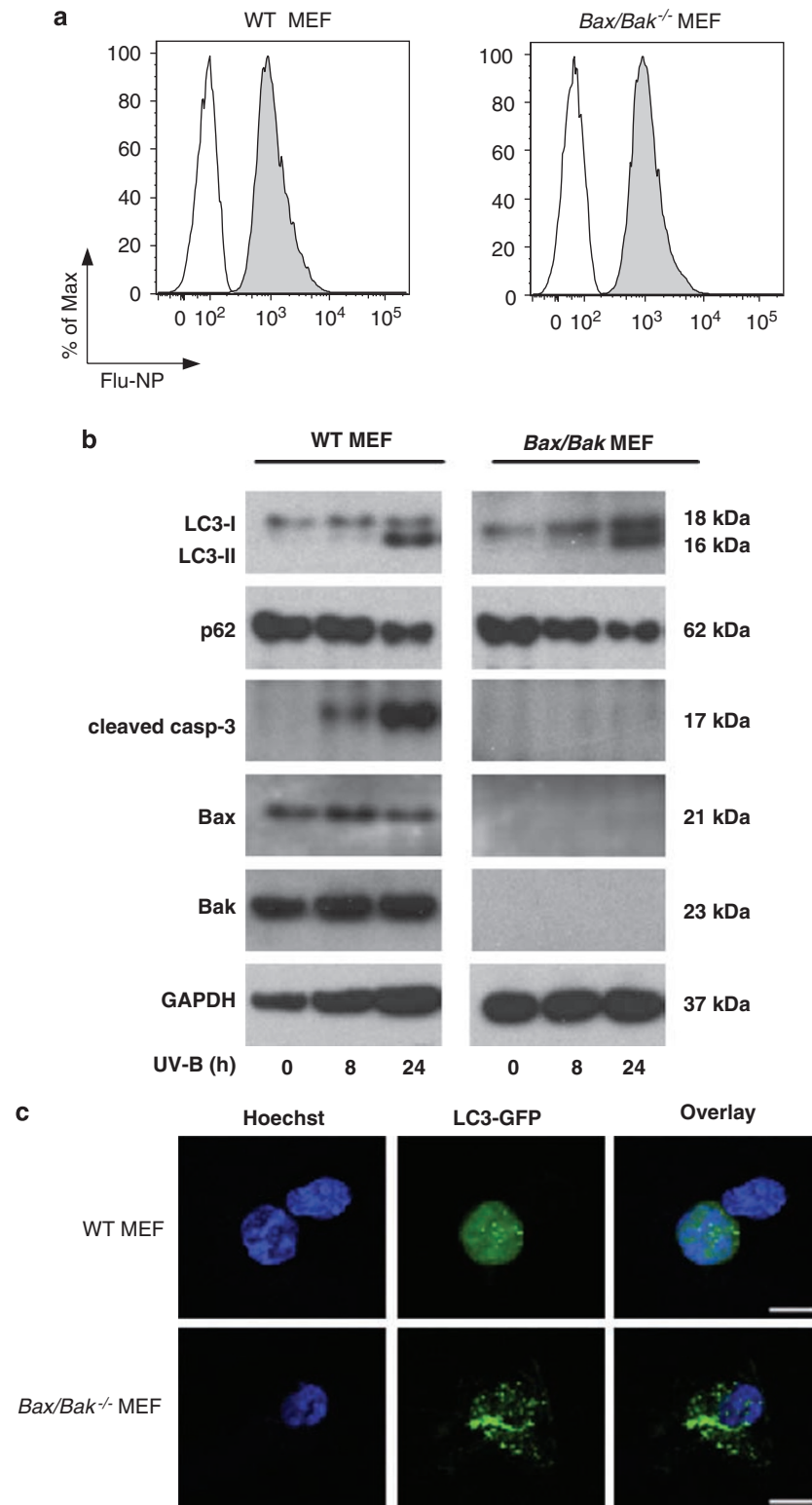
a

b

c

Figure 1 WT and *Bax/Bak*^{−/−} MEFs provide a means of comparing type I and type II programmed death. (**a**) WT and *Bax/Bak*^{−/−} MEFs were infected with influenza A and incubated for 4 h, after which expression of nucleoprotein (NP) was assessed by flow cytometry. (**b**) Influenza-infected WT and *Bax/Bak*^{−/−} MEFs were exposed to 120 mJ/cm^{2} UV-B and after 0, 8 and 24 h, protein lysates were generated and immunoblot analysis was performed. LC3 cleavage, p62 and the cleaved form of caspase-3 were monitored. Bax and Bak expression levels are shown as a control and GAPDH levels were measured to determine protein loading. (**c**) WT and *Bax/Bak*^{−/−} MEFs were transiently transfected with a plasmid encoding for LC3-GFP fusion protein. Cells were exposed to UV-B and after 24 h, punctate staining was assessed by epifluorescence microscopy. A representative image is shown and a high magnification of a single cell illustrates the accumulation of LC3-GFP in autophagosomes. Quantification of the cells is not shown for this experiment, but may be seen for a similar experiment in Figure 3c and Supplementary Figure S2a
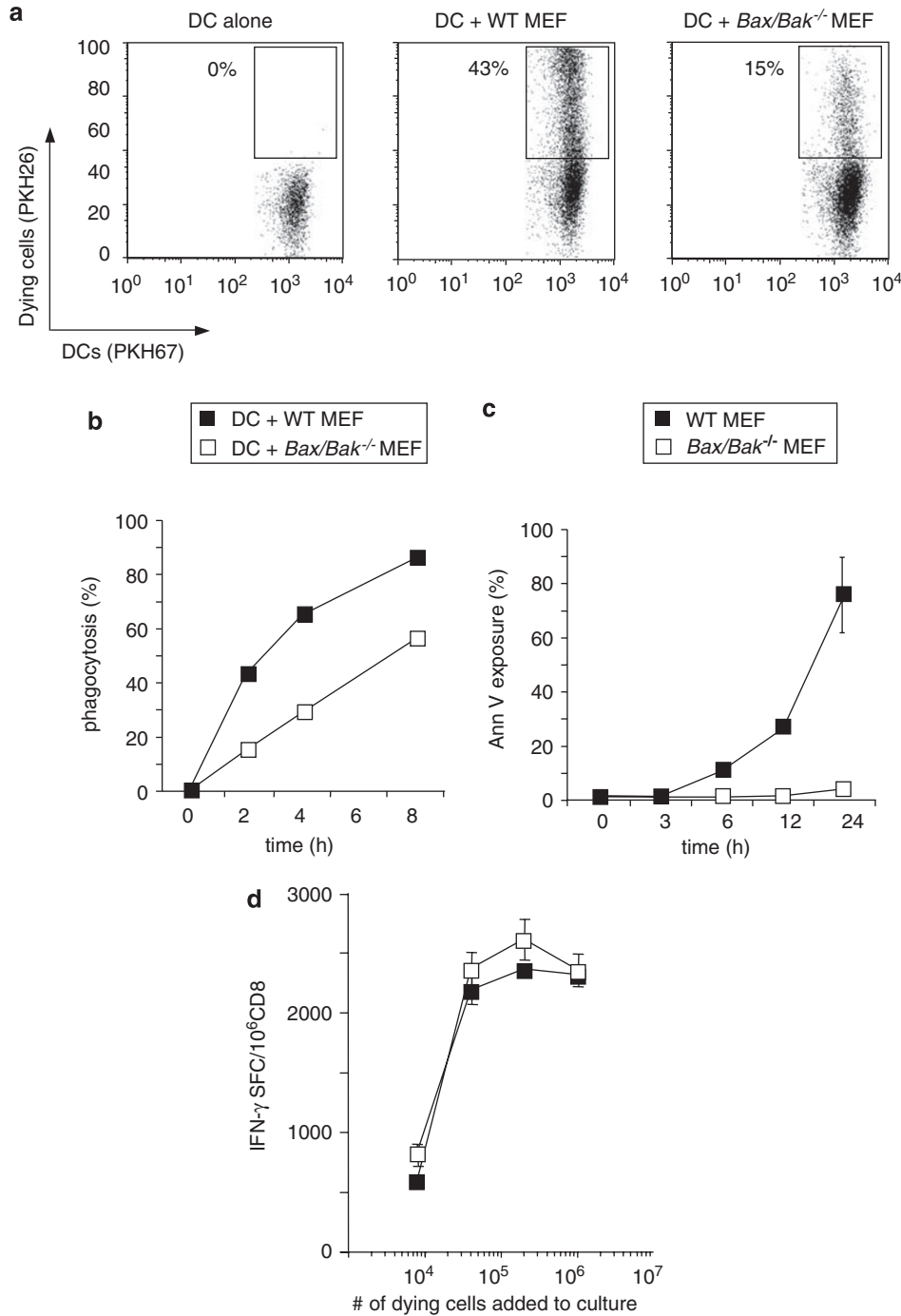
Figure 2 Antigen derived from internalized dead cells is efficiently cross-presented. (**a**, **b**) To assess phagocytosis of dying MEFs, cells were labeled red using the vital dye PKH26 and subsequently exposed to 120 mJ/cm^2 UV-B. After overnight culture, 10^6 monocyte-derived human DCs labeled green using PKH67 were co-cultured with the 10^6 dying WT or *Bax/Bak*$^{-/-}$ MEFs. Using flow cytometry, cells were gated on live DCs, and at 2 h the number of double-positive DCs was determined. A representative FACS plot at the 2 h time point is shown in (**a**). The data from duplicate wells are plotted and S.D. is indicated with bars (**b**). Co-cultures incubated in the presence of EDTA or at 4°C did not reveal the presence of double-positive cells (data not depicted). (**c**) WT and *Bax/Bak*$^{-/-}$ MEFs exposed to UV-B were cultured and at interval time points monitored for exposure of phosphatidylserine (PS) in the outer leaflet of the plasma membrane. PS exposure was monitored by binding of Annexin V-FITC and analyzed by flow cytometry. Averages of triplicate wells are plotted and S.D. is indicated with bars. (**d**) MEF/DC co-cultures were established as above and after 36 h, DCs were purified and exposed to syngeneic polyclonal CD8$^+$ T cells. Influenza-specific IFN-γ-producing CD8$^+$ T cells were monitored by ELISPOT and spot-forming cells (SFCs) are reported. The *x* axis indicates the number of MEFs added to the MEF/DC co-cultures with the DC number fixed at 10^6 cells per well. Values are averages of triplicate wells and error bars indicate standard error. Uninfected MEFs were used as a control and <5 SFCs per 10^6 CD8$^+$ T cells were observed (data not depicted). (**b–d**) Open squares indicate *Bax/Bak*$^{-/-}$ MEFs; filled squares indicate WT MEF. Data are representative of seven experiments

the co-cultures inhibited uptake, and served as a control that double-positive cells are an indicator of phagocytosis by the DCs (data not depicted). Although the *Bax/Bak*$^{-/-}$ MEFs were efficiently captured by the DCs at all time points monitored, the uptake of dying WT MEFs was higher than the *Bax/Bak*$^{-/-}$ MEFs (Figure 2b). We interpreted this result to be a reflection of the kinetics of cell death and the fact that *Bax/Bak*$^{-/-}$ MEFs do not expose phosphatidylserine (PS) to the extent found in WT MEFs and are likely being engulfed through a distinct set of phagocytic receptors (Figure 2c; Ruiz-Vela *et al.*[25] and Wei *et al.*[26]). We next examined the cross-presentation of the internalized antigen. Limiting numbers of influenza-infected UV-B-irradiated MEFs were incubated with human monocyte-derived DCs to determine the efficiency of antigen transfer and T-cell activation. Of note, we have previously demonstrated the ability of human DCs to capture antigen from internalized mouse cells[27] – this approach ensures cross-presentation is the mechanism by which MHC I/peptide complexes are generated. After a 36 h co-culture, DCs were purified based on HLA-DR expression, and tested for the ability to stimulate virus-specific memory CD8$^+$ T-cell responses. An IFN-γ ELISPOT assay was performed and spot-forming cells (SFCs) per 10^6 CD8$^+$ T cells are reported (Figure 2d). Indeed, DCs could process exogenous antigen from cells dying of caspase-mediated and caspase-independent cell death. Importantly, we excluded live virus as the agent responsible for the transfer of antigen to DCs. This was done by confirming that UV-B inactivated the live virus, with the additional precaution of culturing the DCs in human serum containing blocking anti-HA Abs (data not depicted, references report assays performed in similar experimental systems[2,28]). These results indicate that although death and uptake by DCs may be somewhat slower for the *Bax/Bak*$^{-/-}$ MEFs, both cell types are efficient at delivering antigen for cross-presentation. Although these experiments illustrate the ability of type II cell death to permit cross-presentation by human DCs, this experimental system does not permit the evaluation of CD8$^+$ T-cell priming.

Immunization with cells undergoing enhanced autophagy results in robust CD8$^+$ T-cell priming. As compared to re-stimulation of memory cells, which may occur during a 24–36 h time course, the requirements for cross-priming naive CD8$^+$ T cells are more stringent and in some cases require persistent antigen and innate immune activation.[29–31] To evaluate the ability to prime naive T cells, we used an *in vivo* mouse model, injecting dying influenza-infected WT or *Bax/Bak*$^{-/-}$ MEFs by an intradermal (i.d.) route into C57BL/6 mice (H-2^b). Spleens were harvested 14 days post-immunization, CD8$^+$ T cells were purified and the frequency of influenza-specific CD8$^+$ T cells was enumerated using an IFN-γ ELISPOT assay. H-2D^b/NP$_{366-374}$-specific CD8$^+$ T cells were monitored. Strikingly, the *Bax/Bak*$^{-/-}$ MEFs induced more efficient priming (Figure 3a). As the injected MEFs are of C57BL/6 origin we also evaluated priming using Balb/c hosts, thus ensuring that antigen is being cross-presented by host APCs. In the Balb/c model, H-2D^d/HA$_{518-526}$-specific CD8$^+$ T cells were measured and again, we observed a significant difference in the efficiency of priming following immunization

with the *Bax/Bak*$^{-/-}$ MEFs (Figure 3b). In the absence of cognate antigen, the number of IFN-γ-producing CD8$^+$ T cells was below the level of detection.

To further evaluate this phenomenon of enhanced priming, we determined if other inducers of cell death would give a similar result. We first tested staurosporine and etoposide treatment to define which agent would result in a reasonably synchronized population of cells undergoing cell death. On the basis of LC3-GFP punctate staining (Figure 3c), we used etoposide for our functional studies. Confirming our results with UV-B-irradiated cells, we observed enhanced priming when using the *Bax/Bak*$^{-/-}$ MEFs (Figure 3d; data not depicted).

Next, we adoptively transferred CFSE-labeled monoclonal TCR transgenic HA$_{518-526}$-specific CD8$^+$ T cells, called Clone 4 (CL4),[32] thus allowing us to monitor simultaneously cell proliferation (based on dilution of the CFSE dye) and IFN-γ production (using intracellular staining). Following adoptive transfer, Balb/c mice were immunized as above. On day 7 after immunization, draining lymph nodes (DLNs) were harvested and the adoptively transferred T cells were analyzed by flow cytometry (Figure 3e , plots (i) and (ii) and f). In the absence of influenza infection, the CFSE-labeled CL4 cells did not divide and did not produce IFN-γ (Figure 3e, plots (iii) and (iv)). But when antigen-expressing MEFs were used, CL4 division could be detected and after 5–8 cell divisions, IFN-γ production was observed (Figure 3e, plots (v) and (vi)). Given the presence of the adoptively transferred CL4 cells, we do not expect activation of the endogenous repertoire.[33] The percentage of IFN-γ-producing Vβ8.1/2$^+$ CD8$^+$ T cells is plotted as a percentage of the total number of Vβ8.1/2$^+$ CD8$^+$ T cells analyzed (Figure 3f). Supporting our results with the endogenous repertoire, we observed increased numbers of responding CD8$^+$ T cells and higher numbers of IFN-γ-producing CL4 in mice that received cells undergoing autophagy.

We next determined if the difference observed in priming efficiency in the two conditions was a result of the use of the autophagy pathway or the avoidance of death by apoptosis. To distinguish these two possibilities, we performed gene silencing with short-interfering RNA (siRNA) to inhibit Atg5 in the *Bax/Bak*$^{-/-}$ MEFs (Supplementary Figure S1a).[15] We confirmed published data that silencing of Atg5 inhibited autophagy in *Bax/Bak*$^{-/-}$ MEF, causing these cells to ultimately die a necrosis-like cell death (Supplementary Figure S2 and S3)[34]. In addition, we confirmed equivalent influenza antigen expression in the Atg5 knocked-down cells (Supplementary Figure S1b). Notably, silencing of Atg5 rendered the *Bax/Bak*$^{-/-}$ MEFs less efficient in facilitating the cross-priming of influenza-specific CD8$^+$ T cells in both the C57BL/6 and Balb/c models (Figure 4a–c). These experiments establish that antigen transfer following type II PCD results in efficient cross-priming and is dependent on the induction of an Atg5-mediated cascade. Moreover, it demonstrates that for the stimulation of naive CD8$^+$ T cells, cells undergoing autophagy before (or during) cell death are more potent than apoptotic cells. Interestingly, we also observed a decrease in T-cell activation when using Atg5-silenced WT MEFs (Figure 4a and b). Following from the biochemical data that the WT cells are dying while manifesting a mixture of autophagy and apoptotic cell death (Figure 1b), these results
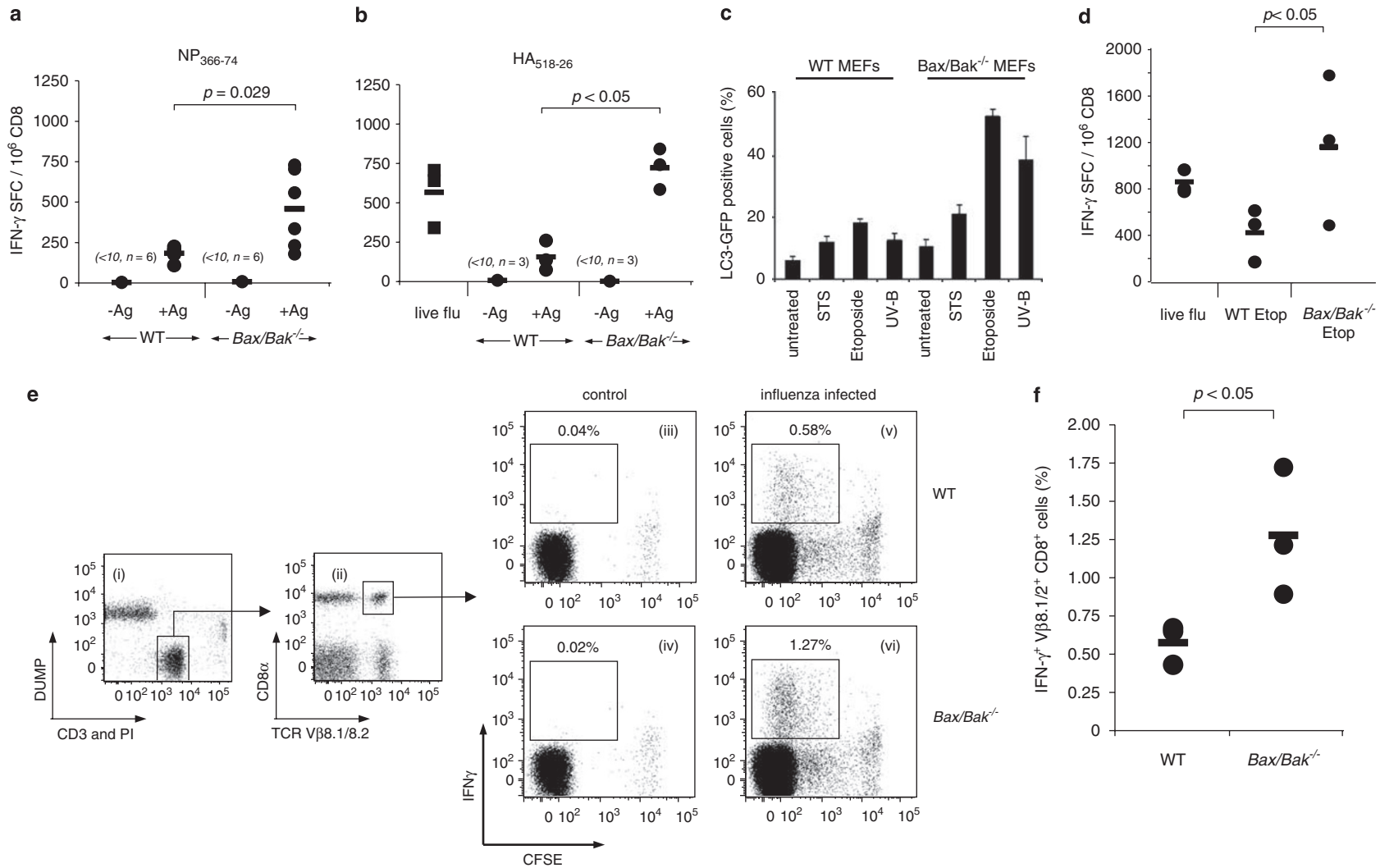
a NP$_{366-74}$

$p = 0.029$

IFN-γ SFC / 10^6 CD8

1250 1000 750 500 250 0

(<10, n = 6) (<10, n = 6)

-Ag +Ag -Ag +Ag

← WT → ← Bax/Bak$^{-/-}$ →

b HA$_{518-26}$

$p < 0.05$

IFN-γ SFC / 10^6 CD8

1250 1000 750 500 250 0

(<10, n = 3) (<10, n = 3)

live flu -Ag +Ag -Ag +Ag

← WT → ← Bax/Bak$^{-/-}$ →

c WT MEFs   Bax/Bak$^{-/-}$ MEFs

LC3-GFP positive cells (%)

60 40 20 0

untreated STS Etoposide UV-B untreated STS Etoposide UV-B

d

$p < 0.05$

IFN-γ SFC / 10^6 CD8

2000 1600 1200 800 400 0

live flu WT Etop Bax/Bak$^{-/-}$ Etop

e

control   influenza infected

0.04% (iii)   0.58% (v)   WT

0.02% (iv)   1.27% (vi)   Bax/Bak$^{-/-}$

(i) DUMP — CD3 and PI

(ii) CD8α — TCR Vβ8.1/8.2

IFNγ — CFSE

f

$p < 0.05$

IFN-γ^+ Vβ8.1/2$^+$ CD8$^+$ cells (%)

2.00 1.75 1.50 1.25 1.00 0.75 0.50 0.25 0

WT Bax/Bak$^{-/-}$

Figure 3 Immunization with Bax/Bak$^{-/-}$ MEFs results in enhanced *in vivo* cross-priming. A total of 10^6 influenza-infected, UV-B-irradiated WT or Bax/Bak$^{-/-}$ MEFs were injected intradermally (i.d.) into C57BL/6 (**a**) or Balb/c mice (**b**). After 14 days, splenocytes were isolated, CD8$^+$ T cells were purified and evaluated for the presence of IFN-γ-producing cells. NP$_{366-374}$/H-2^b- (**a**) and HA$_{518-526}$/H2-D^d (**b**)-specific CD8 T cells were enumerated by ELISPOT. Responses in the absence of antigen (−Ag) were in all cases below the level of detection for the ELISPOT assay. Infection with live influenza was used as a positive control for some of the experiments, and is shown for the priming studies in Balb/c. (**c**) Transfection of cells was performed with an LC3-GFP-expressing plasmid and cells were treated with staurosporine (STS), etoposide or UV-B. After 24 h, cultures were scored for the percentage of cells with LC3-GFP-positive punctae, as described above. On the basis of the data in (**c**), we immunized mice with 10^6 influenza-infected, etoposide (Etop)-treated WT or Bax/Bak$^{-/-}$ MEFs and monitored NP$_{366-374}$/H-2^b CD8$^+$ T-cell priming after 14 days as in (**a**). Data in the Balb/c model showed similar results (not shown). (**e**, **f**) A total of 10^6 CFSE-labeled naive influenza-specific CD8$^+$ T cells (derived from the CL4 transgenic) were adaptively transferred into Balb/c mice. Cross-presentation of HA$_{518-526}$ was monitored 7 days post-immunization. CFSE dilution and intracellular IFN-γ production were monitored by FACS. In (**e**), the gating strategy is shown: we focused on CD3$^+$ cells lacking other lineage markers (indicated by dump). We next chose the subset of CD8α^+ cells utilizing Vβ8.1/2$^+$ as this helped focus our analysis on the transferred CL4 cells. CFSE dilution and intracellular IFN-γ production are shown for control (no influenza) and antigen-expressing MEFs. (**f**) 3/3 mice from a single experiment are shown with the percentage of IFN-γ-positive CD8$^+$ T cells presented as a fraction of the total number of TCR Vβ8.1/2$^+$ cells. (**a**, **b**, **d**, **f**) Individual mice are represented, open circles indicate WT MEF and filled circles indicate Bax/Bak$^{-/-}$ MEFs. Thick bars indicate the mean and statistical significance was evaluated using a Mann–Whitney test, *P*-values are reported. Data are representative of >13 experiments

strengthen our conclusion that autophagy enhances the ability of dying cells to trigger efficient cross-priming as compared to the classical apoptotic pathway(s).

Type II PCD results in more efficient cross-presentation and increased availability of MHC I/peptide complexes. To explain the enhanced priming achieved by the dying $Bax/Bak^{-/-}$ MEFs, we first tested the efficiency and kinetics of antigen cross-presentation by host APCs. As above, we used CFSE-labeled CL4 cells to monitor the presentation of $H2\text{-}D^d/HA_{518-526}$ complexes, with the difference being that we staggered the transfer of the responding T cells. CFSE-labeled CL4 were adoptively transferred on the day of immunization (day 0), day 3, day 6 or day 9 post-immunization and cell division was monitored 3 days after transfer (Figure 5a). T cells isolated from the DLN were analyzed by FACS. In this experiment, the congenic marker Thy1.1 allowed for identification of transferred CL4 cells present in the immunized Thy1.2 Balb/c hosts. Proliferation at the interval time points was determined based on CFSE dilution (Figure 5b) and overlays of the histogram plots allowed comparison between the stimulation achieved in the respective cohorts of mice (Figure 5c, representative mice are shown). The entire data set from a single experiment are shown with proliferation reported as a ratio of divided/total CL4 cells (Figure 5d, open circles, WT MEF; filled circles, $Bax/Bak^{-/-}$ MEF). These cohort studies indicate that there is little proliferation during the first 3 days, which may be explained by the time required for cell death, phagocytosis and DC migration to the DLN. Peak antigen cross-presentation was detected between days 3 and 6 for both groups. At this early time point, responses were equivalent, consistent with the *in vitro* human studies reported above (Figure 2d). Interestingly, immunization with the $Bax/Bak^{-/-}$ MEFs resulted in stronger T-cell stimulation between days 6 and 9, with the CL4 cells being one cell division ahead of those responding to the WT MEFs (Figure 5c). In addition, fewer undivided CL4 cells were observed during the 6- to 9- and 9- to 12-day intervals, indicating that there was the possibility of increased TCR engagement in mice that had received $Bax/Bak^{-/-}$ MEFs as compared to the WT MEFs (Figure 5b–d). To get additional insight into the enhanced priming efficiency, we evaluated additional features that might explain the enhanced immunogenicity of the influenza-infected $Bax/Bak^{-/-}$ MEFs.

$Bax/Bak^{-/-}$ MEFs do not expose calreticulin on the cell surface. To evaluate whether death influenced the immunogenicity at the level of the innate immune response,

we tested whether type II dead cells externalized calreticulin (CRT). It has been demonstrated that one form of 'immunogenic death,' triggered by anthracyclins or UV irradiation, is defined by caspase-dependent exposure of
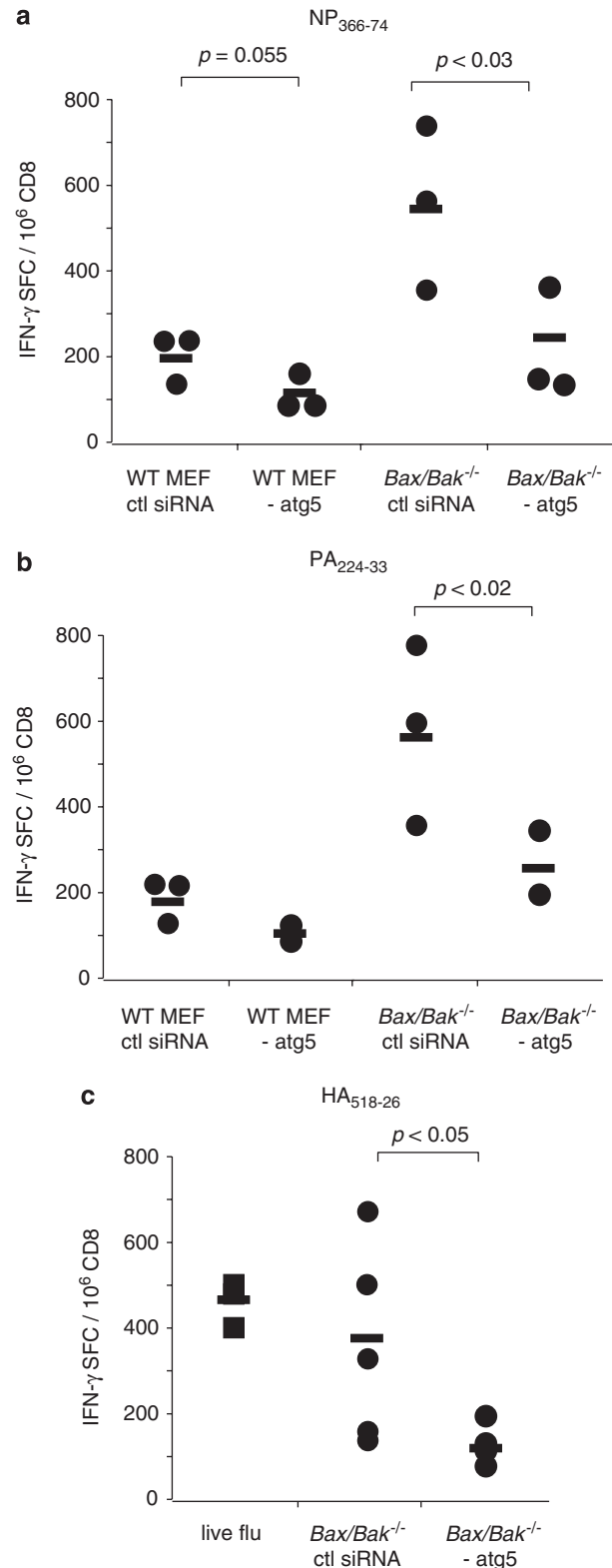
Figure 4 Atg5 expression in dying cells is required for cross-priming of antigen. WT and $Bax/Bak^{-/-}$ MEFs were nucleofected with siRNA directed against Atg5 or a control scrambled siRNA. mRNA expression of Atg5 (targeted mRNA) and beclin-1 (control mRNA) was assessed by quantitative PCR (see Supplementary Figure S1a). These same cells were infected with influenza, exposed to UV-B and injected into C57BL/6 or Balb/c mice. Note, influenza infection was similar in control and siRNA Atg5-silenced cells (see Supplementary Figure S1b). After 14 days, $CD8^+$ T cells reactive for $NP_{366-374}$ (**a**), $PA_{224-233}$ (**b**) or $HA_{518-526}$ (**c**) were enumerated from the respecting strains of mice. Error bars indicate standard error. Data are representative of five experiments

CRT on the cell surface and the release of HMG-B1.[35–37] To evaluate the translocation of CRT during the two forms of cell death, WT and Bax/Bak^{−/−} MEF were exposed to UV-B and surface exposure of CRT was determined by FACS analysis (Figure 6). WT MEFs exposed surface CRT after 6 h, but in contrast Bax/Bak^{−/−} MEF failed to translocate CRT to the cell surface. We also demonstrated that the WT, but not the Bax/Bak^{−/−} MEFs, released HMG-B1 into the supernatant (data not depicted). Further, we evaluated HSP70 expression[38] and did not find evidence of its induction in Bax/Bak^{−/−} MEF (data not depicted). These results indicate that type II PCD represents a distinct form of 'immunogenic death' as it is distinguishable from forms of apoptosis that have been previously shown to be efficient at priming antitumor immune responses.

Autophagy in the antigen donor cell triggers the production of type I IFNs in phagocytic DCs. Recognition of apoptotic cells by DCs may result in the stimulation of pattern recognition receptors and the induction of type I IFNs.[39,40] On the basis of these prior observations, we tested whether the priming efficiency following injection of cells dying with enhanced autophagy could be explained by the induction of IFNα/β. Influenza-infected, UV-B-irradiated MEFs were incubated for 8–10 h to allow for cell death to occur, at which time freshly isolated splenocytes or bone-marrow-derived DCs were added to the cultures. After 24 h, cells were harvested and tested for IFNα2, IFNα4, IFNβ, Mx1, and an interferon-responsive element (IRE) mRNA expression by PCR and culture supernatants were evaluated for IFN-β protein using ELISA. Although the levels of type I IFN mRNA expression were only modestly induced, co-culture of the Bax/Bak^{−/−} MEF with the splenocytes or the bone marrow DCs resulted in a considerable increase in the expression of the IFN-induced genes Mx1 and IRE (Figure 7a and e). This was also evident by the induction of the IFN-induced surface protein BST2, upregulated on DCs that had captured influenza-infected Bax/Bak^{−/−} MEF (Figure 7b). Notably, the induction of the interferon-stimulated genes (ISGs) was dependent on infection of the dying Bax/Bak^{−/−} MEF.

Although only modest levels of IFN mRNA were induced, we did observe >300 pg/ml IFN-β when Bax/Bak^{−/−} MEF were co-cultured with splenocytes (Figure 7c); and 175 × more IFN-β in the Bax/Bak^{−/−} MEF/DC co-cultures as compared to those containing WT MEF (Figure 7f). There were low levels of IFN-β production by the MEFs themselves (Figure 7d), however, this does not account for the levels of cytokine present when splenocytes or DCs were present. Compared to published studies,[40] the level of IFN-β induction that we observed when using the WT MEFs was in a similar

range: 10–30 pg/ml. On the basis of the function of type I IFN, we investigated the levels of MHC I expression on bone-marrow-derived DCs that had captured WT or Bax/Bak^{−/−} MEFs. We observed no significant difference (data not depicted), suggesting that the role of type I IFNs is likely at the level of providing an adjuvant effect for cross-priming.[28,41] Given the robust responses with cells undergoing enhanced autophagy, it suggests that Bax/Bak^{−/−} MEFs could be preserving influenza RNA, thus explaining the stimulation of type I IFNs in phagocytic DCs, which facilitates the observed boost in cross-priming.

To support this hypothesis, we immunized WT and IFNα/β receptor-deficient (IFNAR^{−/−}) C57BL/6 mice using influenza-infected dying Bax/Bak^{−/−} MEF, as per the procedures described above. In the absence of signaling via the IFNAR, there was a marked decrease in the number of IFN-γ-producing CD8^{+} T cells (Figure 8a and b). Together, these data indicate that Bax/Bak^{−/−} MEFs trigger the production of type I IFN, likely by the DCs that engulf them. In turn, this proinflammatory stimulus may enhance the efficiency of antigen cross-priming. In sum, we find that autophagy facilitates efficient antigen cross-priming, which may be explained by sustained TCR engagement and the induction of type I IFNs. These results suggest that use of cells dying by type II PCD would allow for an improved method of achieving cross-priming of viral and possibly tumor-antigen-specific CD8^{+} T cells.

Discussion

Previous studies have shown that apoptotic cells are capable of transferring antigen to DCs, offering a physiologically relevant mechanism whereby exogenous tissue-derived antigen may be presented on the MHC I of a professional antigen-presenting cell.[2] Following this initial study, many investigations compared the efficiency of apoptotic and necrotic cells,[42–46] however only recently have the diversity of cell death pathways and their effect on subsequent immune responses been explored. Here, we developed an experimental system that permitted direct comparison between type I and type II PCD. We utilized paired MEFs, WT versus Bax/Bak^{−/−} cells, which when exposed to the same stressor – UV-B irradiation or etoposide – undergo caspase-mediated and caspase-independent cell death, respectively. Using this model system, we followed the cross-priming of influenza-specific CD8^{+} T cells and demonstrate that T-cell activation following immunization with a single shot of 10[6] cells dying with enhanced autophagy is 3–5 times more efficient than the use of apoptotic cells (Figure 3). These results may in fact be an underestimate as the WT MEFs die while manifesting low levels of autophagy; indeed, when Atg5 is silenced in the WT

Figure 5 Enhanced autophagy in the donor cell permits prolonged cross-presentation of antigen. (**a**) A scheme of the experiment is shown with ' × ' marking the day of Thy1.1[+] CL4 transfer. Mice were immunized on day 0 and staggered cohorts of CFSE-labeled CL4 were used to monitor the presence of H-2D[d]/HA$_{518–526}$. (**b**) Representative FACS plots are shown for each of the respective cohorts. Congenic markers permitted gating on transferred CD8^{+} Thy1.1^{+} CL4 cells present in the Thy1.2^{+} hosts. Boxed cell populations indicate undivided cells. Values indicate the ratio of divided/total CL4 cells. (**c**) CFSE divisions for the same mice from (**b**) are represented by histogram and overlain for ease of comparison between the WT (red lines) and Bax/Bak^{−/−} (blue lines) MEFs. (**d**) Data from the 5/5 mice from a single experiment are shown with individual mice represented. Index of cell is defined as the ratio of divided CL4/total CL4 cells. Data are representative of two independent experiments
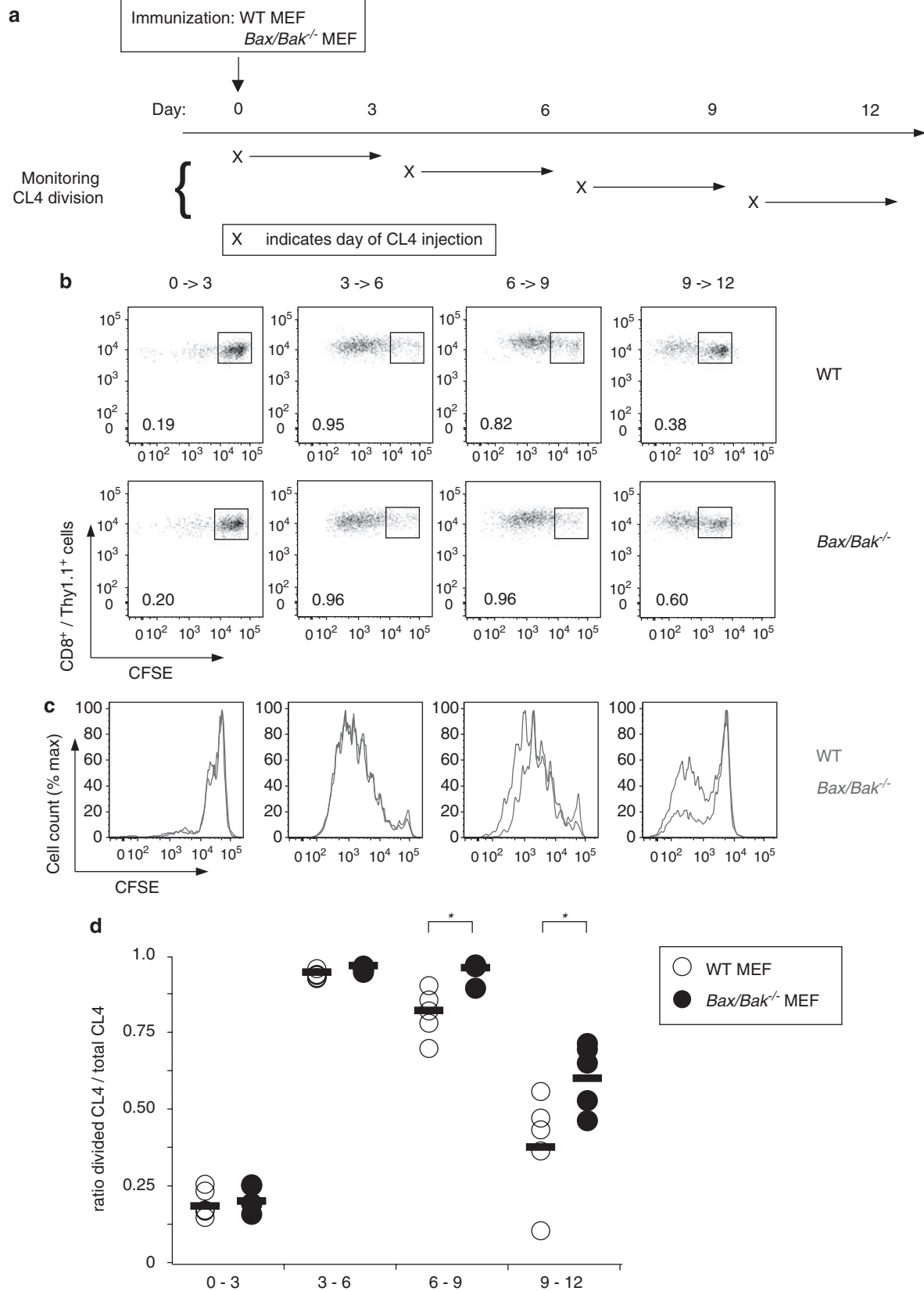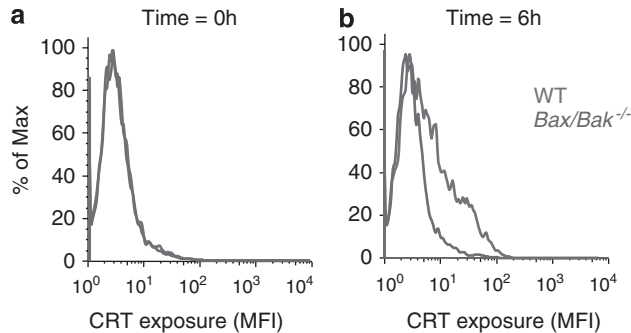
Figure 6 Bax/Bak$^{-/-}$ MEFs do not expose calreticulin (CRT) on the cell surface. CRT exposure was measured in WT and Bax/Bak$^{-/-}$ MEFs at the indicated time points after 120 mJ/m^2 UV-B irradiation. Representative histograms for CRT exposure in live (**a**) and 6 h post-UV-B treated (**b**) cells are shown

cells, we observed reduced priming (Figure 4a and b). Our studies provide the first evidence that enhanced autophagy facilitates the generation and delivery of immunogenic material to DCs. We believe this pathway accounts for the cross-presentation of antigens in situations where apoptosis may be inhibited, for example, tumorigenesis and certain microbial infections. Although autophagy is a physiologic process, it is unclear if it participates in homeostatic cell turnover.[47] Therefore, it remains to be determined whether tolerance to tissue-restricted self-antigens also uses antigen derived from cells undergoing autophagy. Regarding the cross-presentation of viral antigen, our data indicate that, as a consequence of type II cell death, antigens within cells that lack co-stimulatory function for T cells can gain access to the potent DC system, thereby eliciting T-cell responses in a manner that is more robust than previous methods for delivery of cell-associated antigen.

Autophagy and antigen presentation. Although this study represents the first demonstration that antigen may be efficiently cross-presented following the phagocytosis of cells dying with enhanced autophagy, this pathway is not new for the field of antigen presentation.[48,49] Indeed, there is strong evidence that viral, tumor and self-antigens may gain access to the MHC II processing pathway by entry into autophagosomes.[50] This pathway constitutes a mechanism by which endogenous proteins may access the 'classical' exogenous MHC II pathway. Thus far, macroautophagy and chaperone-mediated autophagy have been shown to have a function in the delivery of cytosolic antigen to the MHC II processing. Briefly, macroautophagy involves the enveloping of organelles and cytosolic contents by reticulum-derived membrane, creating double- or multilayered vesicles of 0.5–1.5 μm in diameter. This occurs by the actions of two distinct ubiquitin-like conjugation systems: Atg5–Atg12 and LC3-PE.[51] Alternatively, it has been suggested that LAMP-2a and lysosomal Hsc70 may mediate transport across the lysosomal membrane, permitting cytosolic proteins direct access to the lysosome and the machinery for MHC II antigen processing.[52] Recent data indicate that this mechanism is critical for thymic selection of CD4$^+$ T cells.[53] On the basis of our studies, we implicate macroautophagy as

the dominant means of packaging antigen for cross-presentation, though we cannot rule out the possibility that chaperone-mediated delivery of antigen is important for other classes of cross-presented antigen.

Alternatively, there exists the possibility that Atg5 is participating in autophagy-independent processes that are enhancing delivery to DCs of viral antigen and agonists for the stimulation of IFN production. Two recent studies have identified such autophagy-independent roles for Atg5 and LC3. In the first, Atg5 facilitates the trafficking of an IFN-induced GTPase to the vacuole membrane, thus mediating IFN-γ-directed clearance of Toxoplasma gondii.[54] It has also been reported that LC3 may be recruited to the limiting membrane of phagosomes in a manner that depended on Atg5 yet lacked morphologic features of autophagy.[54] Additional work will be required to determine if the Atg5-mediated enhancement of cross-priming reported here is mechanistically linked to its autophagy or putative autophagy-independent role in cell biologic processes.

Regarding the mechanism(s) by which cells ultimately die when undergoing type II cell death, much remains unknown, but some of the ways in which it differs from apoptosis are instructive and may offer insight into why we observe enhanced cross-priming. One of the key substrates for caspase-3 is the proteasome, and as a result, antigen processing for MHC I presentation is halted as soon as cells commit to apoptosis.[55] In contrast, the proteasome remains functional during caspase-independent cell death. Combined with a delayed kinetics for dying and slower uptake by DCs, there is the possibility that antigen is processed within the dying cell and transferred to DCs, ready for loading onto MHC I. In other words, the autophagosome may contain DRiPs,[56] which may even be protected by chaperones from lysosomal proteases,[22,57] thus increasing the efficiency of antigen transfer. These aspects will be explored in future studies, and may help account for the persistence of MHC I antigen cross-presentation observed when injecting Bax/Bax$^{-/-}$ MEFs (Figure 5).

Autophagy facilitates inflammatory responses. Much less is known concerning how autophagic processes and/or molecules implicated in the autophagy cascade regulate the innate immune system. The published work on the subject is still scarce and seemingly contradictory. Lee et al.[58] reported that induction of autophagy is required for the initial sensing of pathogens by mediating vesicularization of cytosolic viral replication intermediates. In such a manner, viral ssRNA may gain access to the binding domain of TLR7, which typically engages viral nucleic acids that have been internalized through endocytosis. This phenomenon was dependent on active viral replication and expression of Atg5. This seminal study defined a means by which the innate immune system can sense replication of viral genomes in situations in which infection bypasses the endocytic system. In apparent contrast to this study, Jounai et al.[59] have shown that Atg5–Atg12 conjugates negatively regulate type I IFN production by associating with RIG-I and IPS-1 through caspase recruitment domains. One possible explanation is that the viral sensors studied are distinct and that autophagy
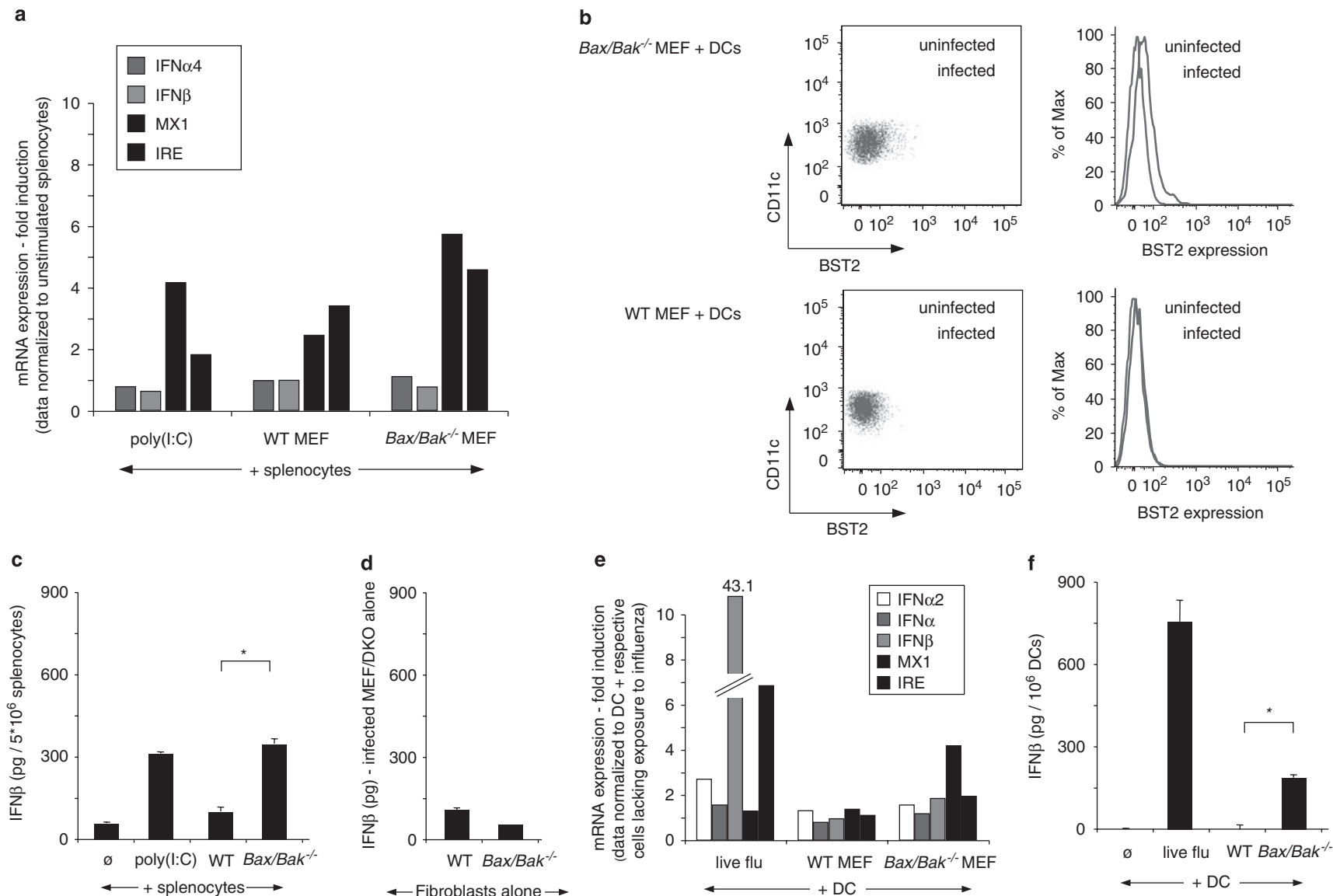
Figure 7 Autophagy in the donor cells stimulates type I interferon (IFN) production in pDCs. (**a**) Dying influenza-infected WT or *Bax/Bak*^{−/−} MEFs were co-cultured with uninfected splenocytes for 24 h. Cells were harvested, RNA extracted, cDNA generated and qPCR performed for IFN-α4, IFN-β and the IFN-induced genes *Mx1* and *IRE*. (**b**) In parallel, we evaluated the upregulation of the IFN-induced surface protein, BST2. Dot-plot overlays and histogram representations are shown for bone-marrow-derived DCs that were co-cultured with WT or *Bax/Bak*^{−/−} MEFs. Infected MEFs are shown in blue, uninfected MEFs in red. (**c**) From the same cultures used in (**a**), supernatants were tested using an IFN-β ELISA. (**d**) As a control, dying influenza-infected WT and *Bax/Bak*^{−/−} MEFs in the absence of splenocytes were tested for mRNA expression (not shown) and IFN-β production. (**e**, **f**) Follow-up experiments were performed using bone-marrow-derived DCs. (**e**) IFN-α4, IFN-α2, IFN-β, Mx1 and IRE mRNA were tested; and (**f**) as above IFN-β ELISA was performed. IFN-α2 (white bars), IFN-α4 (blue bars), IFN-β (green bars), Mx1 (red bars) and interferon response element, IRE (black bars). For mRNA expression data (**a**, **e**), bars represent fold induction as compared to untreated splenocytes or DC. ø indicates DCs alone. *indicates differences that are statistically significant, $P < 0.05$
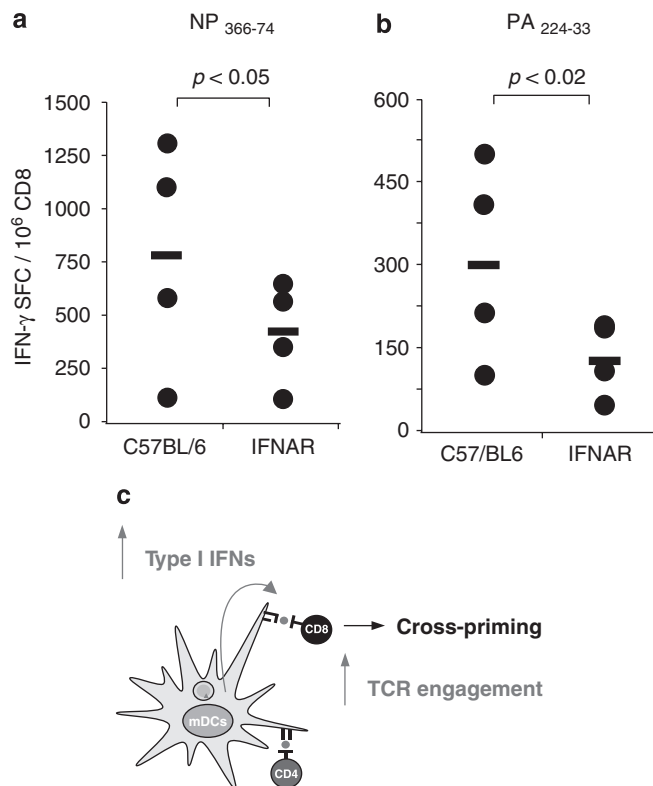
Figure 8 Efficient cross-priming of antigen derived from dying *Bax/Bak*$^{-/-}$ MEFs requires IFNα/β receptor signaling. As above, *Bax/Bak*$^{-/-}$ MEFs were used to immunize WT C57BL/6 or IFNAR$^{-/-}$ mice. After 14 days, NP$_{366-374}$ (**a**) and PA$_{224-233}$ (**b**)-specific CD8$^+$ T cells were enumerated using IFN-γ ELISPOT. Thick bars indicate the mean. Data are representative of two experiments. (**c**) Schematic representation of the mechanisms accounting for how autophagy within the dying cell facilitates enhanced cross-priming by DCs

promotes TLR7 stimulation while downregulating RIG-I/IPS-1 activity. In our study, we used influenza infection as a strategy of viral antigen expression in our donor cells. Although the levels of IFN-β were quite low, we did observe production in WT MEFs, with reduced levels produced by the infected *Bax/Bax*$^{-/-}$ MEFs (Figure 7c). This result is consistent with RIG-I being the sensor for influenza infection in MEFs[60] and with the results of Jounai *et al.*[59] That said, when dying WT and *Bax/Bax*$^{-/-}$ MEFs were incubated with splenocytes or DCs, we observed higher IFN-β and greater induction of ISGs in the latter condition. As it remains unclear if bioactive Atg5–Atg12 conjugates are transferred to the donor cell, and as the sensor responsible for IFN production in the DCs engulfing autophagic cells remains unknown, we cannot precise the reason for the induction of type I IFN in our model system. What is evident is that we observe 50–175 times more IFN-β than that observed when using apoptotic cells (Figure 7; comparison with Janssen *et al.*[40]). Our hypothesis is that viral nucleic acids present in the autophagic corpse are being delivered to the phagosome of the DC, but this possibility will need to be further evaluated.

Utilizing the autophagy pathway to enhance CD8$^+$ T-cell priming. There remains much hope that adoptive immunotherapy will prove a viable option for treating cancer patients and modulating autoimmune disease. Although the data presented here offer exciting insights into immune regu-

lation and novel opportunities for the development of efficient methods of delivering antigens to DCs for cross-presentation, we are aware of the complexity of this biologic process. It is already evident that autophagy may protect cancer cells from the actions of chemotherapy; and ironically, it has also been shown that autophagy may suppress tumorigenesis.[61] Likewise, there are examples of viruses and bacteria that trigger autophagy;[58,62,63] and there are viruses known to inhibit autophagy.[64,65] Unexplored is whether by autophagy, the tumor-/virus-/bacterial-infected cell is participating in recycling their cellular components as a means of countering stress pathways, if it is acting to inhibit innate immunity or if instead it is heading toward type II cell death.

With this significant caveat in mind, we are hopeful that uncovering the mysteries of autophagy will add to our arsenal of strategies for priming antigen-specific CD8$^+$ T-cell responses. Of particular note, there has been interest in the field to combine chemotherapy and immunotherapy with the former triggering cell death that can feed the immune system in a manner that results in T-cell activation. For such purposes, it will be interesting to consider temozolomide as well as other chemotherapeutics that have been shown to trigger nonclassical cell death in malignant cells.[66,67]

In conclusion, our study has expanded the function of Atg5 in the presentation of antigen. For MHC II, autophagy serves as a means of presenting antigen derived from intracellular

microorganisms that manage to evade the endocytic/phago-cytic processing pathway. We find that for cross-presentation autophagy may serve a parallel function, providing a mechanism whereby tissue antigen may be more efficiently transferred from the donor cell to the DCs in situations where microorganisms do not directly infect hematopoietic cells. The utility of this mechanism to develop antitumor and antiviral immunity shows much promise and needs to be evaluated.

Materials and Methods

Reagents. Wild-type and $Bax/Bak^{-/-}$ MEF cells originated from the Korsmeyer Lab (Dana-Farber, Boston, MA, USA) were derived from C57BL/6 mice (H-2^b). Influenza A/PR/8/76 was purchased as purified allantoic fluid from Charles River Laboratories (Spafas, CT, USA) and 250 HAU per 10^6 cells were used for *in vitro* infection; 300 HAU per mouse was used for *in vivo* injections. All FACS Abs were obtained from BD Biosciences Pharmingen (San Diego, CA, USA). FACS analysis was performed on either a BD FACSCalibur or a FACSCanto II and data were exported as *.fcs files analyzed using FlowJo. Immunoblot Abs for cleaved caspase-3 were obtained from Cell Signaling Technologies (Beverly, MA, USA). Abs used in the IFN-γ ELISPOT assays were purchased from Mabtech (Stockholm, Sweden). Poly(I:C) was obtained from InvivoGen (San Diego, CA, USA). Primers for quantitative PCR were provided by Eurogentec (Seraing, Belgium). siRNA directed against Atg5 was purchased from Dharmacon. Immunodominant influenza epitopes: NP$_{366-374}$ and PA$_{224-233}$ (presented by H2-D^b) and HA$_{518-526}$ (presented by H2-D^d) were purchased from NeoMPS (Strasbourg, France). Labeling with CFDA-SE was performed using the Vybrant cell tracer kit from Molecular Probes. PS exposure was measured using the Annexin V-FITC kit from Milteny Biotec (Auburn, CA, USA) following the manufacturer's instruction. Surface CRT was analyzed using rabbit anti-CRT antibody from Abcam (Cambridge, UK) and anti-rabbit IgG (H + L) Alexa Fluor 488 conjugates from Invitrogen (San Diego, CA, USA).

Mice. C57BL/6/J and Balb/c ByJ mice were obtained from Charles River Laboratories, France. CL4 mice, CBy.Cg-Thy1a-Tg(TcraCl4.TcrbCl4) were obtained from the Jackson Laboratory (Bar Harbor, ME, USA). IFN-α/β receptor knockout mice (IFNAR$^{-/-}$) were a kind gift of Deborah Braun. CL4 and IFNAR$^{-/-}$ mice were bred in-house and maintained in a helicobacter-free SPF facility, and used at an age of 6–15 weeks under approved protocols.

Isolation and preparation of human DC and CD8 T cells. PBMCs were isolated from whole blood by sedimentation over Ficoll-Hypaque (Amersham Pharmacia Biotech, Piscataway, NJ, USA). DCs were prepared from the T-cell-depleted fraction (sheep cell rosetting) by culturing cells in the presence of 1000 U/ml GM-CSF (Berlex, Seattle, WA, USA) and 500–1000 U/ml IL-4 (R&D Systems, Minneapolis, MN, USA) for 6 days. To generate mature DCs, cultures were stimulated with 50 ng/ml TNF-α (Alexis Biochemicals, Lausen, Switzerland) and 0.1 μM PGE2 (Sigma, St. Louis, MO, USA) for 36–48 h. At days 6–7, more than 95% of the cells were CD14$^-$ CD83$^-$ HLA-DR^{low} DCs. After maturation, on days 8–9, 70–95% of the cells were of the mature CD14$^-$ CD83$^+$ HLA-DR^{hi} phenotype. DCs were purified to more than 99% purity after co-culture with apoptotic cells based on expression of HLA-DR; and primary CD8 T cells were purified using anti-CD8 Abs coupled to iron particles and passage through the magnetic activated cell sorting (MACS) column purification system (Miltenyi Biotech, Auburn, CA, USA).

Human studies: monitoring phagocytosis and cross-presentation. WT and $Bax/Bak^{-/-}$ MEFs were dyed red using PKH26-GL (Sigma) and induced to undergo death by UV-B irradiation with 120 mJ/cm^2. After 24 h, allowing the cells to undergo death, human monocyte-derived immature DCs were dyed green with PKH67-GL (Sigma) and added to the co-culture. After 1, 2, 4 and 8 h, FACS analysis was carried out and double-positive cells were enumerated. For functional studies, 2×10^5 purified CD8$^+$ T cells were added to 6.7×10^3 purified HLA-DR^{++} DCs to give a ratio of 30 : 1 (T-cell/DC ratio). The cultures were incubated in 96-well plates precoated with a capture antibody for IFN-γ. After 24–36 h, cells were washed out with mild detergent and a biotin-conjugated IFN-γ mAb was added to the wells, followed by exposure to HRP-based detection reagents from the Vectastain Elite kit (Vector Laboratories, Burlingame, CA, USA). Colored spots indicated the cells that had released IFN-γ and data are reported as

SFCs/10^6 CD8 T cells. Data from triplicate wells were averaged and mean data are reported. The ELISPOT plate evaluation was performed in a blinded fashion by an independent service (Zellnet Consulting Inc., New York, NY, USA) using an automated ELISPOT reader (Carl Zeiss Inc., Thornwood, NY, USA) with KS Elispot 4.8 software.

Mouse studies: immunization and monitoring influenza-specific T-cell responses. WT and $Bax/Bak^{-/-}$ MEFs were infected with influenza A/PR/8 for 1 h and washed extensively. After an additional 4–6 h to allow for expression of viral antigens, cells were exposed to 120 mJ/cm^2 UV-B. Before injection, cells were washed again and resuspended in PBS at the concentration of 10^7 cells per ml. Injections were performed through the i.d. route using a volume of 100 μl. To monitor priming efficiency, spleens were harvested 12–14 days after immunization and CD8$^+$ T cells were purified using the MACS purification strategies (Miltenyi Biotech). ELISPOT assays were allowed for enumeration of IFN-γ-producing cells as described above. For mouse cultures, 2×10^5 T cells were co-cultured with 6.7×10^3 mature bone-marrow-derived DCs that had been pulsed with 10 μM peptide. For intracellular IFN-γ staining of adoptively transferred CFSE-labeled CL4 cells, experiments were performed 7 days after immunization.

Western analysis. Lysates were prepared in 150 mM NaCl, 50 mM Tris-HCl (pH 8), 1% NP-40, 0.5% DOC, 0.03% sodium dodecyl sulfate (SDS), 2 mM EDTA. Total protein was determined by Lowry's method and 10–20 μg was loaded on a 4–12% gradient SDS–polyacrylamide gel electrophoresis (Invitrogen). Proteins were transferred to PVDF membrane and blotted with indicated Abs. Secondary HRP-coupled Abs were detected using ECL Plus (Amersham Pharmacia Biotech).

siRNA knockdown. WT and $Bax/Bak^{-/-}$ MEFs (2.5×10^6) were transfected with siRNA (10 μg siRNA per 10^6 cells) using the Amaxa electroporation system according to the manufacturer's protocol (kit V, program U-20). The electroporation efficiency was $>75\%$, assessed by co-transfection with DNA-expressing GFP. The siRNA sequences used were as follows (numbers in parentheses indicate nucleotide positions within the respective open reading frame): siRNA mouse atg5: 5′-CGAAUUCCAACUUGCUUUAUU-3′ (42–60); siRNA mouse atg5: 5′-GCAUAAAAGUCAAGUGAUCUU-3′ (407–425). Quantitative PCR was performed to confirm siRNA knockdown and for both probes $>80\%$ silencing was achieved.

Quantitative PCR. RNA was extracted using TRIZOL (Invitrogen, Carlsbad, CA, USA) and cDNA was synthesized from 1 to 2 μg RNA using oligo-dT (Roche, Indianapolis, IN, USA) and Superscript reverse transcriptase (Invitrogen) according to the manufacturer's instruction. Atg5- and beclin-1-specific mRNA was quantified relative to β-actin with SYBRGreen incorporation. The primers used were as follows: atg5 forward, 5′-GACAGATTTGACCAGTTTTGGGC-3′; atg5 reverse, 5′-GGGTTTCCAGCATTGGCTCTATC-3′; beclin-1 forward, 5′-GGAAAAGAACCGCA AGGTGGTG-3′; beclin-1 reverse, 5′-AAACTGTCCGCTGTGCCAGATG-3′; β-actin forward, 5′-TAGACTTCGAGCAGCAGGAGGAGATG-3′; β-actin reverse, 5′-CGTA CTACTGCTTGCTGATCCA-3′. IFN-β, IFN-α_4, IFN-α_2, Mx1 and IRE were monitored using set of primers and probes identified and purchased from Applied Biosystems: Mm00439546_s1, Mm00833969_s1, Mm00833961_s1, Mm00487796_m1, Mm00499068_m1, respectively. The reactions were run on a PTC200 equipped with a Chromo4 detector (MJ Research, Watertown, MA, USA). The analyses were performed with Opticon Monitor software version 2.03. All the measurements were performed in duplicate and validated when the difference in C_t between the two measures was less than 0.3. The ratio gene of interest to housekeeping gene was calculated according to the formula: ratio $= 2 - C_t$ (CT $=$ mean C_t gene $-$ mean C_t housekeeping).

Determining persistence of H2-D^d/HA$_{518-526}$ complexes within immunized recipients. CL4 cells (Thy1.1) were isolated from spleen and lymph nodes and labeled with 5 μM CFSE in PBS. After extensive washing in ice-cold PBS, 2×10^5 CL4 CD8$^+$ T cells were injected intravenously into Thy1.2 immunized female recipients. Cohorts were staggered as described in the text and 3 days after injection, the DLN was harvested and analyzed. Mice were processed independently and cells were labeled with CD8–PE CD3-PerCP-Cy5.5 and Thy1.1-APC Abs allowing for the identification of the transferred CL4 CD8$^+$ T cells and the determination of CFSE intensity.

1. Albert ML. Death-defying immunity: do apoptotic cells influence antigen processing and presentation? *Nat Rev Immunol* 2004; **4**: 223–231.
2. Albert ML, Sauter B, Bhardwaj N. Dendritic cells acquire antigen from apoptotic cells and induce class I-restricted CTLs. *Nature* 1998; **392**: 86–89.
3. Casares N, Pequignot MO, Tesniere A, Ghiringhelli F, Roux S, Chaput N et al. Caspase-dependent immunogenicity of doxorubicin-induced tumor cell death. *J Exp Med* 2005; **202**: 1691–1701.
4. Bevan MJ. Cross-priming for a secondary cytotoxic response to minor H antigens with H-2 congenic cells which do not cross-react in the cytotoxic assay. *J Exp Med* 1976; **143**: 1283–1288.
5. Savill J, Dransfield I, Gregory C, Haslett C. A blast from the past: clearance of apoptotic cells regulates immune responses. *Nat Rev Immunol* 2002; **2**: 965–975.
6. Albert ML, Pearce SF, Francisco LM, Sauter B, Roy P, Silverstein RL et al. Immature dendritic cells phagocytose apoptotic cells via alphavbeta5 and CD36, and cross-present antigens to cytotoxic T lymphocytes. *J Exp Med* 1998; **188**: 1359–1368.
7. Stuart LM, Lucas M, Simpson C, Lamb J, Savill J, Lacy-Hulbert A. Inhibitory effects of apoptotic cell ingestion upon endotoxin-driven myeloid dendritic cell maturation. *J Immunol* 2002; **168**: 1627–1635.
8. Kim S, Elkon KB, Ma X. Transcriptional suppression of interleukin-12 gene expression following phagocytosis of apoptotic cells. *Immunity* 2004; **21**: 643–653.
9. Voll RE, Herrmann M, Roth EA, Stach C, Kalden JR, Girkontaite I. Immunosuppressive effects of apoptotic cells [letter]. *Nature* 1997; **390**: 350–351.
10. Maiuri MC, Zalckvar E, Kimchi A, Kroemer G. Self-eating and self-killing: crosstalk between autophagy and apoptosis. *Nat Rev Mol Cell Biol* 2007; **8**: 741–752.
11. Thornberry NA, Lazebnik Y. Caspases: enemies within. *Science* 1998; **281**: 1312–1316.
12. Strasser A. The role of BH3-only proteins in the immune system. *Nat Rev Immunol* 2005; **5**: 189–200.
13. Perfettini JL, Kroemer G. Caspase activation is not death. *Nat Immunol* 2003; **4**: 308–310.
14. Zitvogel L, Casares N, Pequignot MO, Chaput N, Albert ML, Kroemer G. Immune response against dying tumor cells. *Adv Immunol* 2004; **84**: 131–179.
15. Shimizu S, Kanaseki T, Mizushima N, Mizuta T, Arakawa-Kobayashi S, Thompson CB et al. Role of Bcl-2 family proteins in a non-apoptotic programmed cell death dependent on autophagy genes. *Nat Cell Biol* 2004; **6**: 1221–1228.
16. Codogno P, Meijer AJ. Autophagy and signaling: their role in cell survival and cell death. *Cell Death Differ* 2005; **12** (Suppl 2): 1509–1518.
17. Furuya N, Yu J, Byfield M, Pattingre S, Levine B. The evolutionarily conserved domain of Beclin 1 is required for Vps34 binding, autophagy and tumor suppressor function. *Autophagy* 2005; **1**: 46–52.
18. Gutierrez MG, Munafo DB, Beron W, Colombo MI. Rab7 is required for the normal progression of the autophagic pathway in mammalian cells. *J Cell Sci* 2004; **117**: 2687–2697.
19. Petrovski G, Zahuczky G, Katona K, Vereb G, Martinet W, Nemes Z et al. Clearance of dying autophagic cells of different origin by professional and non-professional phagocytes. *Cell Death Differ* 2007; **14**: 1117–1128.
20. Kepp O, Rajalingam K, Kimmig S, Rudel T. Bak and Bax are non-redundant during infection- and DNA damage-induced apoptosis. *EMBO J* 2007; **26**: 825–834.
21. Lindsten T, Thompson CB. Cell death in the absence of Bax and Bak. *Cell Death Differ* 2006; **13**: 1272–1276.
22. Blachere NE, Darnell RB, Albert ML. Apoptotic cells deliver processed antigen to dendritic cells for cross-presentation. *PLoS Biol* 2005; **3**: e185.
23. Klionsky DJ, Abeliovich H, Agostinis P, Agrawal DK, Aliev G, Askew DS et al. Guidelines for the use and interpretation of assays for monitoring autophagy in higher eukaryotes. *Autophagy* 2008; **4**: 151–175.
24. Kabeya Y, Mizushima N, Ueno T, Yamamoto A, Kirisako T, Noda T et al. LC3, a mammalian homologue of yeast Apg8p, is localized in autophagosome membranes after processing. *EMBO J* 2000; **19**: 5720–5728.
25. Ruiz-Vela A, Opferman JT, Cheng EH, Korsmeyer SJ. Proapoptotic BAX and BAK control multiple initiator caspases. *EMBO Rep* 2005; **6**: 379–385.
26. Wei MC, Zong WX, Cheng EH, Lindsten T, Panoutsakopoulou V, Ross AJ et al. Proapoptotic BAX and BAK: a requisite gateway to mitochondrial dysfunction and death. *Science* 2001; **292**: 727–730.
27. Albert ML, Jegathesan M, Darnell RB. Dendritic cell maturation is required for the cross-tolerization of CD8+ T cells. *Nat Immunol* 2001; **2**: 1010–1017.
28. Longman RS, Braun D, Pellegrini S, Rice CM, Darnell RB, Albert ML. Dendritic-cell maturation alters intracellular signaling networks, enabling differential effects of IFN-alpha/beta on antigen cross-presentation. *Blood* 2007; **109**: 1113–1122.
29. Jusforgues-Saklani H, Uhl M, Blachère N, Lemaître F, Lantz O, Bousso P et al. Antigen persistence is required for dendritic cell licensing and CD8+ T cell cross-priming. *J Immunol* 2008; **181**: 3067–3076.
30. Curtsinger JM, Johnson CM, Mescher MF. CD8 T cell clonal expansion and development of effector function require prolonged exposure to antigen, costimulation, and signal 3 cytokine. *J Immunol* 2003; **171**: 5165–5171.
31. Bevan MJ. Helping the CD8(+) T-cell response. *Nat Rev Immunol* 2004; **4**: 595–602.
32. Morgan DJ, Liblau R, Scott B, Fleck S, McDevitt HO, Sarvetnick N et al. CD8(+) T cell-mediated spontaneous diabetes in neonatal mice. *J Immunol* 1996; **157**: 978–983.
33. Badovinac VP, Haring JS, Harty JT. Initial T cell receptor transgenic cell precursor frequency dictates critical aspects of the CD8(+) T cell response to infection. *Immunity* 2007; **26**: 827–841.
34. Colell A, Ricci JE, Tait S, Milasta S, Maurer U, Bouchier-Hayes L et al. GAPDH and autophagy preserve survival after apoptotic cytochrome *c* release in the absence of caspase activation. *Cell* 2007; **129**: 983–997.
35. Obeid M, Tesniere A, Ghiringhelli F, Fimia GM, Apetoh L, Perfettini JL et al. Calreticulin exposure dictates the immunogenicity of cancer cell death. *Nat Med* 2007; **13**: 54–61.
36. Obeid M, Panaretakis T, Joza N, Tufi R, Tesniere A, van Endert P et al. Calreticulin exposure is required for the immunogenicity of gamma-irradiation and UVC light-induced apoptosis. *Cell Death Differ* 2007; **14**: 1848–1850.
37. Apetoh L, Ghiringhelli F, Tesniere A, Obeid M, Ortiz C, Criollo A et al. Toll-like receptor 4-dependent contribution of the immune system to anticancer chemotherapy and radiotherapy. *Nat Med* 2007; **13**: 1050–1059.
38. Feng H, Zeng Y, Whitesell L, Katsanis E. Stressed apoptotic tumor cells express heat shock proteins and elicit tumor-specific immunity. *Blood* 2001; **97**: 3505–3512.
39. Schulz O, Diebold SS, Chen M, Naslund TI, Nolte MA, Alexopoulou L et al. Toll-like receptor 3 promotes cross-priming to virus-infected cells. *Nature* 2005; **433**: 887–892.
40. Janssen E, Tabeta K, Barnes MJ, Rutschmann S, McBride S, Bahjat KS et al. Efficient T cell activation via a toll–interleukin 1 receptor-independent pathway. *Immunity* 2006; **24**: 787–799.
41. Le Bon A, Et N, Rossmann C, Ashton M, Hou S, Gewert D et al. Cross-priming of CD8(+) T cells stimulated by virus-induced type I interferon. *Nat Immunol* 2003; **4**: 1009–1015.
42. Gallucci S, Lolkema M, Matzinger P. Natural adjuvants: endogenous activators of dendritic cells [in process citation]. *Nat Med* 1999; **5**: 1249–1255.
43. Sauter B, Albert ML, Francisco L, Larsson M, Somersan S, Bhardwaj N. Consequences of cell death. Exposure to necrotic tumor cells, but not primary tissue cells or apoptotic cells, induces the maturation of immunostimulatory dendritic cells. *J Exp Med* 2000; **191**: 423–434.
44. Basu S, Binder RJ, Suto R, Anderson KM, Srivastava PK. Necrotic but not apoptotic cell death releases heat shock proteins, which deliver a partial maturation signal to dendritic cells and activate the NF-kappa B pathway. *Int Immunol* 2000; **12**: 1539–1546.
45. Larsson M, Fonteneau JF, Somersan S, Sanders C, Bickham K, Thomas EK et al. Efficiency of cross presentation of vaccinia virus-derived antigens by human dendritic cells. *Eur J Immunol* 2001; **31**: 3432–3442.
46. Scheffer SR, Nave H, Korangy F, Schlote K, Pabst R, Jaffee EM et al. Apoptotic, but not necrotic, tumor cell vaccines induce a potent immune response *in vivo*. *Int J Cancer* 2003; **103**: 205–211.
47. Levine B, Kroemer G. Autophagy in the pathogenesis of disease. *Cell* 2008; **132**: 27–42.
48. Munz C. Autophagy and antigen presentation. *Cell Microbiol* 2006; **8**: 891–898.
49. Paludan C, Schmid D, Landthaler M, Vockerodt M, Kube D, Tuschl T et al. Endogenous MHC class II processing of a viral nuclear antigen after autophagy. *Science* 2005; **307**: 593–596.
50. Schmid D, Munz C. Innate and adaptive immunity through autophagy. *Immunity* 2007; **27**: 11–21.
51. Mizushima N, Noda T, Yoshimori T, Tanaka Y, Ishii T, George MD et al. A protein conjugation system essential for autophagy. *Nature* 1998; **395**: 395–398.
52. Cuervo AM, Dice JF. A receptor for the selective uptake and degradation of proteins by lysosomes. *Science* 1996; **273**: 501–503.
53. Nedjic J, Aichinger M, Emmerich J, Mizushima N, Klein L. Autophagy in thymic epithelium shapes the T-cell repertoire and is essential for tolerance. *Nature* 2008; **455**: 396–400.
54. Zhao Z, Fux B, Goodwin M, Dunay IR, Strong D, Miller BC et al. Autophagosome-independent essential function for the autophagy protein Atg5 in cellular immunity to intracellular pathogens. *Cell Host Microbe* 2008; **4**: 458–469.
55. Adrain C, Creagh EM, Cullen SP, Martin SJ. Caspase-dependent inactivation of proteasome function during programmed cell death in *Drosophila* and man. *J Biol Chem* 2004; **279**: 36923–36930.
56. Yewdell JW, Bennink JR. Cut and trim: generating MHC class I peptide ligands. *Curr Opin Immunol* 2001; **13**: 13–18.
57. Binder RJ, Srivastava PK. Peptides chaperoned by heat-shock proteins are a necessary and sufficient source of antigen in the cross-priming of CD8+ T cells. *Nat Immunol* 2005; **6**: 593–599.
58. Lee HK, Lund JM, Ramanathan B, Mizushima N, Iwasaki A. Autophagy-dependent viral recognition by plasmacytoid dendritic cells. *Science* 2007; **315**: 1398–1401.
59. Jounai N, Takeshita F, Kobiyama K, Sawano A, Miyawaki A, Xin KQ et al. The Atg5 Atg12 conjugate associates with innate antiviral immune responses. *Proc Natl Acad Sci USA* 2007; **104**: 14050–14055.
60. Kato H, Takeuchi O, Sato S, Yoneyama M, Yamamoto M, Matsui K et al. Differential roles of MDA5 and RIG-I helicases in the recognition of RNA viruses. *Nature* 2006; **441**: 101–105.
61. Marx J. Autophagy: is it cancer's friend or foe? *Science* 2006; **312**: 1160–1161.
62. Birmingham CL, Smith AC, Bakowski MA, Yoshimori T, Brumell JH. Autophagy controls *Salmonella* infection in response to damage to the *Salmonella*-containing vacuole. *J Biol Chem* 2006; **281**: 11374–11383.

63. Nakagawa I, Amano A, Mizushima N, Yamamoto A, Yamaguchi H, Kamimoto T *et al.* Autophagy defends cells against invading group A *Streptococcus. Science* 2004; **306**: 1037–1040.
64. Talloczy Z, Jiang W, Virgin IV HW, Leib DA, Scheuner D, Kaufman RJ *et al.* Regulation of starvation- and virus-induced autophagy by the eIF2alpha kinase signaling pathway. *Proc Natl Acad Sci USA* 2002; **99**: 190–195.
65. Jackson WT, Giddings Jr TH, Taylor MP, Mulinyawe S, Rabinovitch M, Kopito RR *et al.* Subversion of cellular autophagosomal machinery by RNA viruses. *PLoS Biol* 2005; **3**: e156.
66. Kanzawa T, Germano IM, Komata T, Ito H, Kondo Y, Kondo S. Role of autophagy in temozolomide-induced cytotoxicity for malignant glioma cells. *Cell Death Differ* 2004; **11**: 448–457.
67. Green DR, Kroemer G. Pharmacological manipulation of cell death: clinical applications in sight? *J Clin Invest* 2005; **115**: 2610–2617.

Supplementary Information accompanies the paper on Cell Death and Differentiation website (http://www.nature.com/cdd)